Transient Weakening of Earth's Magnetic Shield Probed by a Cosmic Ray Burst

P. K. Mohanty, K. P. Arunbabu, T. Aziz, S. R. Dugad, S. K. Gupta,*
B. Hariharan, P. Jagadeesan, A. Jain, S. D. Morris, and B. S. Rao
Tata Institute of Fundamental Research, Homi Bhabha Road, Mumbai 400005, India†

Y. Hayashi and S. Kawakami
Graduate School of Science, Osaka City University, 558-8585 Osaka, Japan†

A. Oshima and S. Shibata
College of Engineering, Chubu University, Kasugai, Aichi 487-8501, Japan†

S. Raha
Bose Institute, 93/1, A.P.C. Road, Kolkata 700009, India†

P. Subramanian
Indian Institute of Science Education and Research, Pune 411021, India†

H. Kojima
Faculty of Engineering, Aichi Institute of Technology, Toyota City, Aichi 470-0392, Japan†
(Received 16 June 2016; published 20 October 2016)

The GRAPES-3 tracking muon telescope in Ooty, India measures muon intensity at high cutoff rigidities (15–24 GV) along nine independent directions covering 2.3 sr. The arrival of a coronal mass ejection on 22 June 2015 18:40 UT had triggered a severe G4-class geomagnetic storm (storm). Starting 19:00 UT, the GRAPES-3 muon telescope recorded a 2 h high-energy (∼20 GeV) burst of galactic cosmic rays (GCRs) that was strongly correlated with a 40 nT surge in the interplanetary magnetic field (IMF). Simulations have shown that a large (17×) compression of the IMF to 680 nT, followed by reconnection with the geomagnetic field (GMF) leading to lower cutoff rigidities could generate this burst. Here, 680 nT represents a short-term change in GMF around Earth, averaged over 7 times its volume. The GCRs, due to lowering of cutoff rigidities, were deflected from Earth's day side by ∼210° in longitude, offering a natural explanation of its night-time detection by the GRAPES-3. The simultaneous occurrence of the burst in all nine directions suggests its origin close to Earth. It also indicates a transient weakening of Earth's magnetic shield, and may hold clues for a better understanding of future superstorms that could cripple modern technological infrastructure on Earth, and endanger the lives of the astronauts in space.

DOI: 10.1103/PhysRevLett.117.171101

Introduction.—The geomagnetic field (GMF) [1] shields Earth from energetic charged particles by deflecting them away over several Earth radii (R_E) [2]. Eruptive solar processes produce coronal mass ejections (CMEs) that are large plasma structures with embedded turbulent magnetic fields, that are ejected into the heliosphere from the solar corona [3]. The space weather is driven by these CMEs that can have profound societal impact by triggering severe storms that disrupt space, and ground-based communication. The largest storm in recorded history was the famous Carrington event of 1859 that disrupted a relatively robust communication system of telegraph lines of that era for several hours [4,5]. However, the occurrence of a similar event today could cripple the suite of smart devices including mobile phones, computer networks, etc., on Earth, and satellites in space. This is due to the widespread use of VLSI circuits in these devices, which may not survive the high radiation environment produced by a Carrington-like event [6,7].

The reconfiguration of the magnetic field through reconnection is the key to interpret the energy release in coronal mass ejections (CMEs), and the generation of solar magnetic field through dynamo action [8]. The magnetic field, and associated turbulence in the CMEs causes slow (∼days) reduction in the galactic cosmic ray (GCR) intensity called Forbush decrease (FD) events [9–12]. The CMEs containing a southward directed IMF induce reconnection, whereby, the magnetic field ahead of Earth's bow shock is "opened up" [13] producing storms [14,15]. The GMF shields Earth by deflecting GCRs away, resulting in a threshold, termed "cutoff rigidity," below which GCRs cannot reach Earth [16]. Episodes of increase in the GCR intensity due to decrease in the cutoff rigidity "R_c" during storms have also been reported earlier [2,17,18].

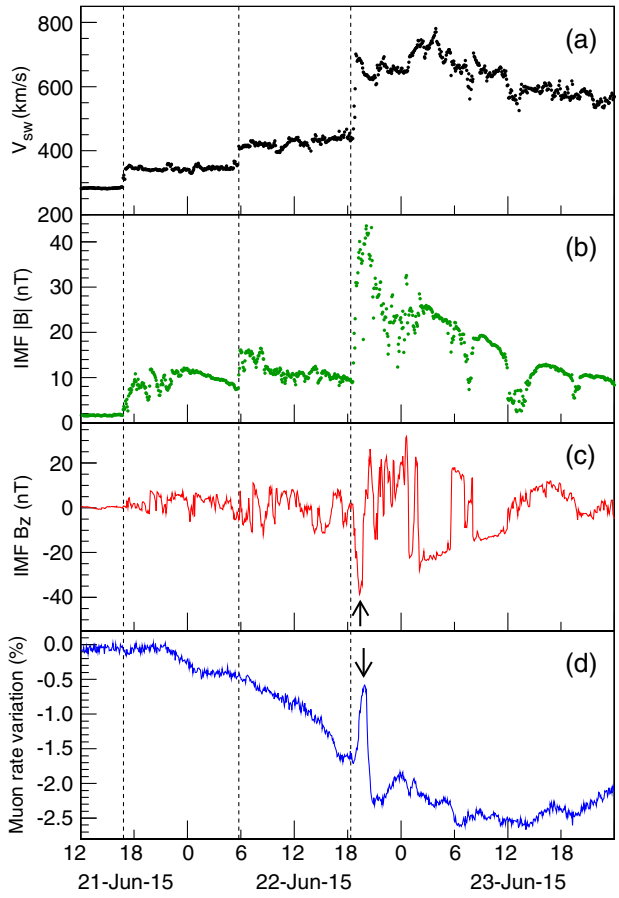

FIG. 1. Top 3 panels show WIND data time shifted to the bow-shock nose: (a) V_{SW}, (b) $|B|$, (c) B_z, (d) GRAPES-3 muon-rate. Vertical dashed lines indicate CME arrival times (UT).

On 21 June 2015, a symmetric full-halo CME erupted from the sunspot region NOAA 2371 associated with a double peaked M2-class solar flare. It appeared in the SOHO/LASCO C2 images at 02:36 UT, and reached Earth on 22 June 2015 18:40 UT, and triggered a severe G4-class storm producing radio blackouts, and Aurore Borealis [19]. Two preceding CMEs had arrived on 21 June 2015 16:45 UT, and 22 June 2015 05:45 UT, respectively, and both had originated from the same sunspot region. The CME parameters, including the solar wind speed (V_{SW}), magnetic field $|B|$, and B_z its component perpendicular to the ecliptic plane, measured by the WIND spacecraft (at L1, 1.5×10^6 km from Earth) are available on OMNIWeb [20]. The WIND data, time shifted to the bow-shock nose already accounted for propagation delay from the spacecraft [21] available on OMNIWeb, were used here. In Figs. 1(a) and 1(b) the arrival of the three CMEs are marked by jumps in V_{SW}, and $|B|$, respectively. For 2 h, the passage of the third CME enhanced $|B|$ to 44 nT (Fig. 1b), and B_z to -40 nT [Fig. 1(c)].

Burst detection by GRAPES-3.—The large area (560 m^2) GRAPES-3 tracking muon telescope in Ooty, India, due to its near-equatorial location, experiences high cutoff rigidities (15–24 GV). It measures the muon intensity along nine independent directions in the sky by detecting ≥ 1 GeV muons produced by the GCRs in the atmosphere [22,23]. Thus, the muons serve as proxies for GCRs, and hence the terms "muon rate," and "GCR intensity" (GCRI) will be used interchangeably. The nine muon directions are labeled NE(northeast), N, NW, E, V(vertical), W, SE, S, SW (southwest) in a 2.3 sr field of view, as listed in Fig. 3. The GRAPES-3 detects 1.5×10^8 muons per hour, which provides an accurate estimate of the GCRI variation [23–25]. The muon rate is corrected for instrumental and atmospheric pressure variations [26]. The corrected muon rates are yet modulated by the solar diurnal anisotropy (SDA) at a frequency of 1 cycle per day (cpd), and to a lesser extent by two higher harmonics. By the use of a fast Fourier transform (FFT) based filter, SDA can be largely eliminated. However, the use of FFT requires observed data to be converted into an uninterrupted time series of 2^N intervals, where N is a positive integer. Accordingly, the muon rates measured every four min for $2^{13} = 8192$ intervals spanning 23 days from 12 June 2015 18:28 UT to 4 July 2015 12:36 UT were used here. To remove the contribution of SDA on the muon rate, the FFT spectrum was subjected to a smooth filter to reject frequencies from 0.5 to 3.5 cpd. The inverse FFT of the filtered spectrum yielded a muon rate free from the influence of SDA as shown in Fig. 1(d) [10,26].

As seen from Fig. 1(d), an FD was in progress 4.5 h after the arrival of first CME on 21 June 16:45 UT. In the midst of this FD, a 2 h muon burst (19:00–21:00 UT) correlated with B_z is clearly seen from Fig. 1(d), and Fig. 1(c), respectively, as indicated by the arrows. Another FFT filter

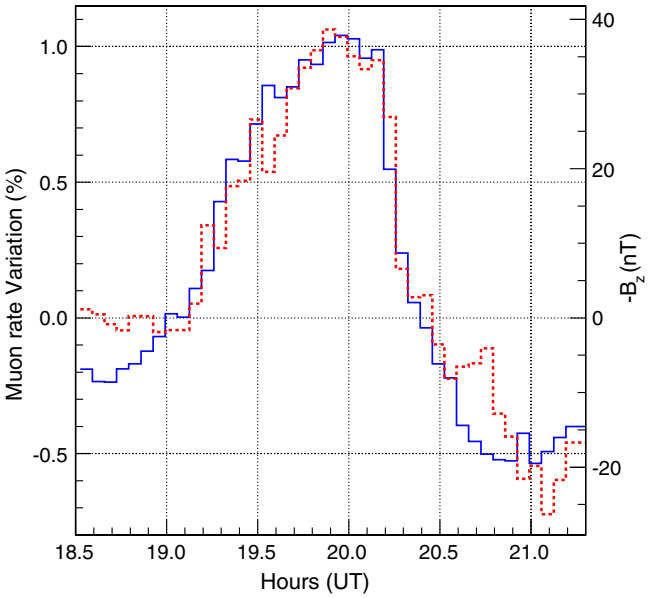

FIG. 2. Muon-rate (solid line) and $-B_z$ (broken line) on 22 June 2015, correlation coefficient $R = -0.94$.

was used to eliminate the frequencies < 0.5 cpd to remove the slow FD contributions. The muon data now contain only frequencies > 3.5 cpd. The muon rate, and $-B_z$, data at 4 min resolution are shown in Fig. 2. B_z was delayed by 32 min which maximized its correlation with the muon data to $R = -0.94$, highlighting the intimate connection of the GCRI on Earth, and the B_z in space. Every 4 min, $\sim 10^6$ muons are detected in each of the nine directions, resulting in a statistical error of $\sim 0.1\%$. Thus, an excess of 9.2×10^5 on a background of 2.9×10^8 muons during this 2 h interval implies a significance in excess of 50σ.

The nine muon profiles obtained after inverse FFT are shown by the solid lines in Fig. 3. The burst amplitudes show a gradual decline from north (N = 1.8%) to south (SW = 0.8%) directions. Each direction shows a simultaneous GCRI surge from 19:00 UT, reaching a maximum at 20:00 UT. For an interplanetary phenomenon, the expected time offset between V, and directions NE, E, SE is -100 min. Similarly, the offset between V, and NW, W, SW is 100 min based on the 25° angle between them. However, the observed offsets between V, and NE, E, SE, NW, W, SW, measured via a cross correlation yielded a mean of (-3 ± 4) min, consistent with a value of zero within the 4 min time resolution. As expected, the time offsets between V, and N, S were also zero. Thus, the near simultaneity of the GCR burst in all directions strongly suggests its origin close to Earth, possibly within the magnetosphere.

Simulation of GCR burst.—We tested the hypothesis that the burst was generated by a sudden lowering of the cutoff rigidities by recalculating R_c for a GMF perturbed via reconnection with the IMF. The telescope field of view was

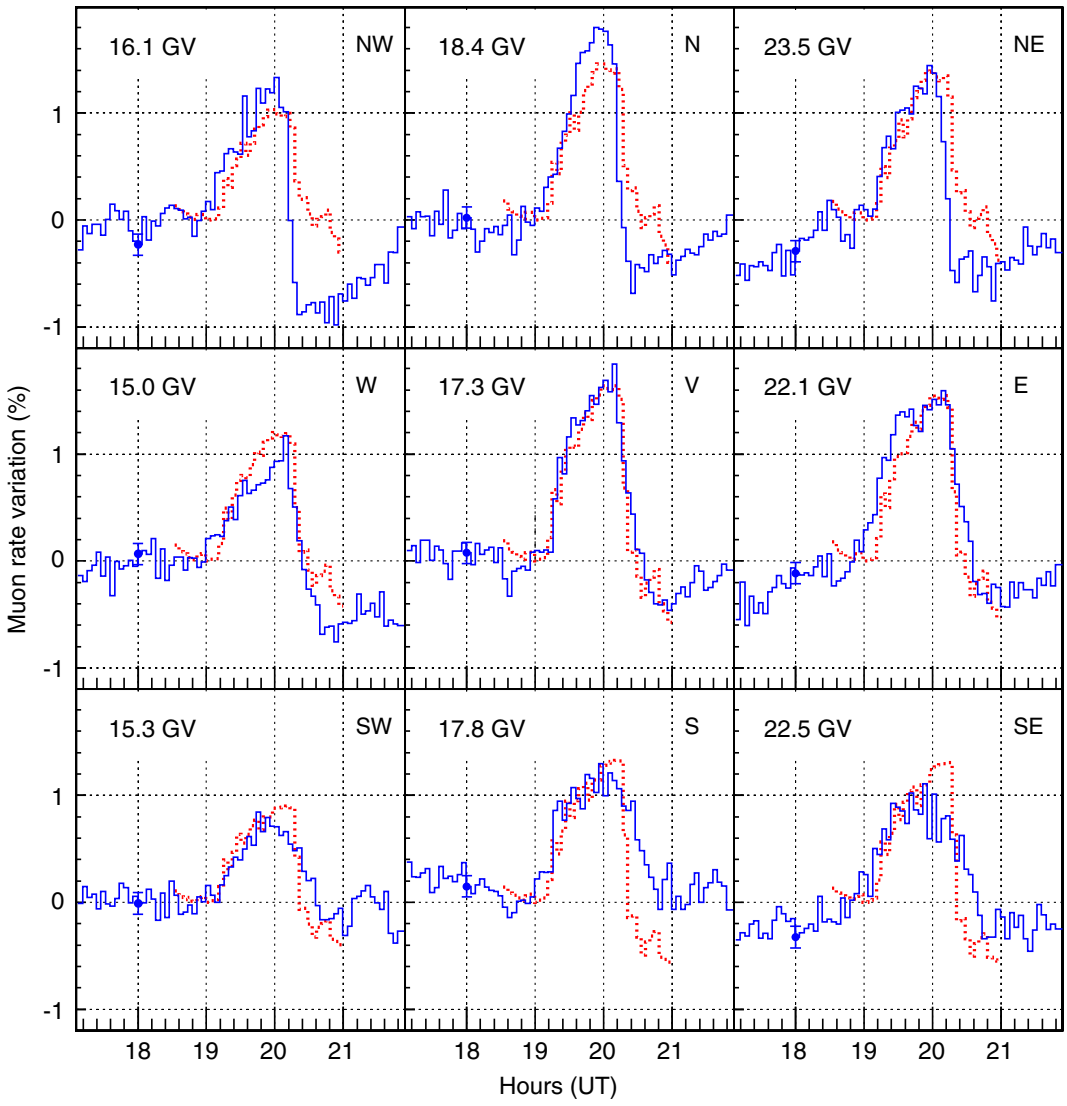

FIG. 3. Muon-rate variation in nine directions observed by GRAPES-3 on 22 June 2015 shown by the solid line. Simulation results normalized to data by scaling the IMF 17 times are shown by the broken line. Cutoff rigidities (GV) and error bars are shown for each direction.

divided into 360° × 60° grid, each 1° in azimuth and zenith directions. In a magnetic field, the trajectory of protons arriving at Earth is the same as that of antiprotons ($\bar{p}$) of the same rigidity leaving Earth. Thus, to simulate the proton trajectories, $\bar{p}$ of increasing rigidity moving away from Earth were launched from each grid point. Their trajectories were traced to a distance "D" [16] in a GMF modeled by IGRF-11 [27], after adding the IMF (B_x, B_y, B_z averaged every 4 min) to the respective GMF components. The smallest rigidity $\bar{p}$ escaping Earth defines the R_c for that direction. Equivalently, a proton of R_c would be the lowest rigidity particle to reach Earth from outer space along the same trajectory. We varied D from 1.5 to $25R_E$, and found that R_c gradually reduced and reached its asymptotic value at $D = 2R_E$, which was used thereafter.

The production of muons in the atmosphere due to interaction of GCRs above R_c was simulated by Monte Carlo code CORSIKA [28]. The simulated muons satisfying the trigger requirements of the muon telescope were binned into the nine directions mentioned above. The difference between the muon rates before, and after adding the IMF was calculated for every 4 min. The interval 18:40–19:00 UT was used as the baseline to estimate the change in rates both for the data, as well as simulations. The simulated amplitudes were significantly smaller (∼0.05%) than the measured (∼1.0%) ones. These simulations were repeated after enhancing the IMF by a factor $2 < f < 20$. The results obtained showed that the amplitudes scaled with f. A simultaneous minimization of χ^2 for the nine pairs of observed, and simulated profiles yielded $f = 17$.

The nine simulated profiles are shown in Fig. 3 by broken lines. Very high correlations (-0.89 ± 0.05) between the measured, and simulated profiles are seen in all nine cases. The reduction in R_c varied from 0.5 in the south to 0.7 GV in the north. It is remarkable that a simple model with a common compression factor $f = 17$ ($B_z = -680$ nT) reproduced the amplitude, and the shapes of all nine profiles quite well. Since the burst was caused by a decrease of the GMF out to $D = 2R_E$, thus, this decrease of 680 nT, was averaged over a volume of $(2^3\text{-}1) = 7V_E$ surrounding Earth where V_E is the volume of Earth.

The GCRs near the cutoff experience **a** large deflection in the GMF. To estimate this "deflection," asymptotic directions were calculated for 5×10^4 protons. Protons of rigidities from R_{ci} to $R_{ci} + \Delta R_{ci}$ GV for $i = 1, 9$ directions were simulated. Here ΔR_{ci}, were the changes in the respective cutoff rigidities (0.5–0.7 GV). Trajectories for the most probable rigidity for the nine directions, viewed from the north pole are shown in Fig. 4(a). These trajectories are bending 195°–230°; thus, the asymptotic directions lie in the opposite hemisphere. In Fig. 4(b) an equatorial view of these trajectories is shown. Thus, the GCRs producing the muon burst detected on the night side were deflected ∼210° from the day side.

Discussion.—The frozen-in, IMF component $-B_z = 40$ nT could be enhanced via compression of the CME-sheath region. During this storm, Earth's bow-shock nose was compressed from 11.4 to $4.6R_E$ [20]. The implied reduction in the area suggests that $-B_z$ would have been enhanced by a factor $(11.4/4.6)^2 = 6.14$. Additionally, assuming the CME shock to be quasiperpendicular, it could further enhance B_z by a factor < 4 [29]. Thus, $-B_z = 40$ nT measured at L1, could, in principle, be enhanced by a factor $< 4 \times 6.14 = 24.6$ to < 980 nT. Thus, the reduction of 680 nT possibly induced by reconnection with the GMF, was ∼70% of its maximum possible value.

An examination of the worldwide neutron monitor data showed that Almaty, and Nor-Amberd stations located on the night side recorded increased rates coincident with GRAPES-3. However, no significant increase was seen by the instruments on the day side [30]. The 32 min delay of the burst relative to the IMF could be due to the GCRs diffusing across a turbulent IMF [11,12]. The long-term changes in the GMF are typically measured from satellites [1]; however, GCRs provide an inexpensive and yet reliable probe of the short-term changes in the GMF over a large volume ($7V_E$). The fortuitous location of GRAPES-3 on the night side, opposite to the reconnection site on the day side, enabled the detection of this burst. The burst had

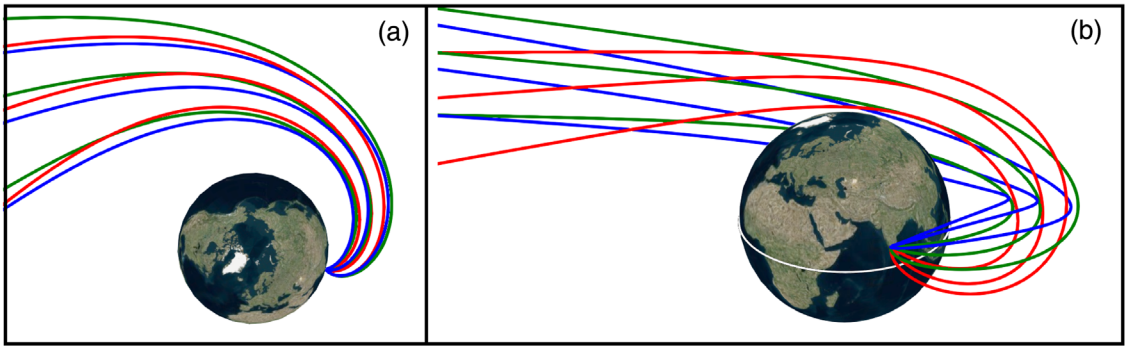

FIG. 4. GCR trajectories near the cutoff rigidity responsible for the burst viewed from the (a) north pole and (b) the equator. NW, N, NE shown in blue, W, V, E in green, SW, S, SE in red.

occurred due to reduction of the cutoff rigidities from a temporary reconnection-induced 680 nT decrease in the GMF with a relatively high efficiency of 70%. The near simultaneity of the burst in all nine directions indicates its origin close to Earth. The N-S gradient in the amplitudes (1.8:1) of the burst was caused by the relative alignment of $-B_z$ with respective directions. Any alternative explanation involving enhancement of the GCR intensity due to IMF is not feasible due to the negative correlation between these two variables. The occurrence of this burst also implies a 2 h weakening of Earth's protective magnetic shield during this event. This burst allowed observation of the annihilation of the magnetic field arising from reconnection in a large volume surrounding Earth by the novel probe of GCRs. Depending on the orbital variation of the cutoff rigidities, the astronauts on the International Space Station (ISS) would have received a high, and variable radiation dose during the burst. The AMS detector on the ISS [31] is ideally located to further investigate this burst, and its effects on astronauts onboard. This event may also hold clues to the impact of superstorms that may occur in the future.

Conclusions.—The GRAPES-3 muon telescope in Ooty, India detected a 2 h burst of GCRs starting 22 June 2015 19:00 UT that was strongly correlated with a 40 nT surge in the IMF. Monte Carlo simulations showed compression of IMF to 680 nT spread over 7 times Earth's volume, and subsequent reconnection with the GMF leading to lower cutoff rigidities may have generated this burst. A $\sim 210°$ bending of the GCRs due to lowering of cutoff rigidities resulted in detection of this day-side burst on the night side by the GRAPES-3. The occurrence of the burst indicates a 2 h transient weakening of Earth's magnetic shield, which may hold clues for a better understanding of future superstorms.

We thank D. B. Arjunan, G. P. Francis, V. Jeyakumar, S. Kingston, K. Manjunath, S. Murugapandian, B. Rajesh, K. Ramadass, V. Santoshkumar, C. Shobana, and R. Sureshkumar for their help in running the experiment. We gratefully acknowledge access to the Neutron-Monitor Database of the European Union.

*gupta.crl@gmail.com
†The GRAPES-3 Experiment, Cosmic Ray Laboratory, Raj Bhavan, Ooty 643001, India.

[1] N. Olsen *et al.*, Geophys. Res. Lett. **42**, 1092 (2015).
[2] L. I. Dorman, *Cosmic Rays in Magnetosphere of Earth and Planets* (Springer, New York, 2009), ISBN .
[3] D. F. Webb and T. A. Howard, Living Rev. Solar Phys. **9**, 3 (2012).
[4] R. C. Carrington, Mon. Not. R. Astron. Soc. **20**, 13 (1859).
[5] Y. D. Liu *et al.*, Nat. Commun. **5**, 3481 (2014).
[6] *Severe Space Weather Events–Understanding Societal and Economic Impacts: A Workshop Report* (National Academies Press, Washington, 2008) doi:10.17226/12507.
[7] http://www.oecd.org/gov/risk/46891645.pdf.
[8] E. Priest and T. Forbes, *Magnetic Reconnection* (Cambridge University Press, Cambridge, England, 2007), ISBN 978-0-521-03394-7.
[9] H. V. Cane, Space Sci. Rev. **93**, 55 (2000).
[10] P. Subramanian *et al.*, Astron. Astrophys. **494**, 1107 (2009).
[11] K. P. Arunbabu, H. M. Antia, S. R. Dugad, S. K. Gupta, Y. Hayashi, S. Kawakami, P. K. Mohanty, T. Nonaka, A. Oshima, and P. Subramanian, Astron. Astrophys. **555**, A139 (2013).
[12] K. P. Arunbabu, H. M. Antia, S. R. Dugad, S. K. Gupta, Y. Hayashi, S. Kawakami, P. K. Mohanty, A. Oshima, and P. Subramanian, Astron. Astrophys. **580**, A41 (2015).
[13] C. S. Arridge *et al.* Nat. Phys. **12**, 268 (2016).
[14] X. H. Deng and H. Matsumoto, Nature (London) **410**, 557 (2001).
[15] H. U. Frey, T. D. Phan, S. A. Fuselier, and S. B. Mende, Nature (London) **426**, 533 (2003).
[16] D. F. Smart and M. A. Shea, Adv. Space Res. **36**, 2012 (2005).
[17] I. Kondo, J. Phys. Soc. Japan Suppl. A **17**, 402 (1962).
[18] S. Kudo, M. Wada, P. Tanskanen, and M. Kodama, J. Geophys. Res. **92**, 4719 (1987).
[19] http://cdaw.gsfc.nasa.gov/CME_list/halo/halo.html;http://www.swpc.noaa.gov/noaa-scales-explanation.
[20] http://omniweb.gsfc.nasa.gov/form/omni_min.html.
[21] L. F. Bargatze R. L. McPherron, J. Minamora and D. Weimer, J. Geophys. Res. **110**, A07105 (2005).
[22] Y. Hayashi *et al.*, Nucl. Instrum. Methods Phys. Res., Sect. A **545**, 643 (2005).
[23] T. Nonaka *et al.*, Phys. Rev. D **74**, 052003 (2006).
[24] H. Kojima *et al.*, Astropart. Phys. **62**, 21 (2015).
[25] H. Kojima *et al.*, Phys. Rev. D **91**, 121303(R) (2015).
[26] P. K. Mohanty *et al.*, *Proc. Sci.*, (ICRC2015) 045; P. K. Mohanty *et al.*, Astropart. Phys. **79**, 23 (2016).
[27] C. Finlay *et al.*, Geophys. J. Int. **183**, 1216 (2010).
[28] https://www.ikp.kit.edu/corsika/.
[29] R. M. Kulsrud, *Plasma Physics for Astrophysics* (Princeton University Press, Princeton, NJ, 2004), ISBN: 978-0691120737.
[30] http://www.nmdb.eu.
[31] http://www.ams02.org.